

Application and technological research of the "Trifid" system - the synergy of cooperation in the R&D area

Roman Kaczyński*, Grzegorz Mieczkowski*, Adam Ławicki**

* Białystok University of Technology, ul. Wiejska 45C, 15-351 Białystok, Poland

**White Hill Sp. z o.o., ul. Żurawia 71 lok 3.08, 15-540 Białystok, Poland

e-mail: r.kaczynski@pb.edu.pl,

Abstract: The article presents the project of the structural part of the "Trifid" system. The system consists of an autonomous vehicle with a mechanical platform. The main object of the "Trifid" system is to gather and transmit plant data to a control centre, where based on the image analysis, the decisions of applying appropriate intervention are made.

Keywords: Lifting mechanisms, mobile robot, design

1. Introduction

The use of an innovative method of obtaining and analysing information on the state of plants grown together with the autonomous platform moving around greenhouses is an innovative solution on a global scale. The use of such a system can be a breakthrough transition from the analysis of plants by humans to continuous observation and research of plants by robots. It will revolutionize the production of greenhouse vegetables in Europe and in the world, contributing to the competitiveness of the entire industry, but also will increase the competitiveness of robot manufacturers.

The platform is made of a base on which additional drives, controlling a platform lifting mechanism to the assumed height of 6m, are mounted. Directly on the base, the platform lifting mechanism is also mounted. The vision system, used for gathering and transmission plant data, is mounted on the top of the lifting mechanism.

In order to optimize the weight of the vehicle and platform, the necessary strength calculations (analytical and numerical) were made. Mechanical connections, bearings, belts, etc. with the use analytical techniques were calculated. For the rest elements, based on the technical parameters of the "Trifid" system and documentation prepared in the SolidWorks environment, numerical analyses (finite element method) were carried out. Distribution of displacements and reduced stresses (according to the Huber-Mises hypothesis) were obtained in the form of chromatic maps. What is more, the traction properties and stability conditions of both the autonomous vehicle and platform were determined. The obtained results are presented in the next sections

of this paper. Since the lifting mechanism plays an important role in the "Trifid" platform, a brief literature review of such mechanisms is presented below.

2. Lifting mechanisms review

Lifting mechanisms are widely used in many areas of the economy, such as industry, agriculture, defence or telecommunications [1, 2]. Construction assumptions of the lifting mechanism of "Trifid" platform are close to those used in communication. These are movable masts of antennas or telemetry pieces of equipment applied, for example in meteorology. It is worth to pay special attention to telescopic poles (fig. 1) because of their weight and the possibility of minimizing the dimensions while maintaining the desired functions.



Fig. 1. Telescopic mast [2]

In the project under analysis, besides the load placed on the platform, it is also important to provide energy and cabling for data transmission. One of the

proposals is to put automatically push-pull cable inside the mast. Such a solution, although very desirable, requires the preparation of an internal sealed channel and a dedicated coiler machine.

Noteworthy is a solution characterized by the simplicity of routing cables outside the mast (fig. 2). The use of a shape memory material allows for easy fitting of cabling's length during mast operation. The sealing of the actuator segments and the servicing and possible replacement of the cable are also facilitated. Another way of arranging the wiring harness are cable guides (fig. 3) which are used in machine tools.



Fig. 2. Cables with shape memory [2]



Fig. 3. The cable guide [2]

Due to the small lift load (weight not exceeding 5 kg), a simple way of the mast movement, it is proposed to use a telescopic structure with a mechanically or pneumatically powered. Because of the considerable height of lifting (about 6 m), it may be necessary to use a different structure than telescopic what more detailed was discussed in section 4.

3. Kinematic aspects of the "Trifid" platform

The assumptions of the project relate to the mechanical construction of the robot and predict lifting a load of 5 kg (vision system with cabling) to a height of 6 m. The dimensions of the vehicle should be in a rectangle 800 mm wide and 1500 mm long. It is also assumed that the vehicle can cross obstacles up to 150 mm high with the mast laid down. Figure 4 presents a prototype of the vehicle and base.

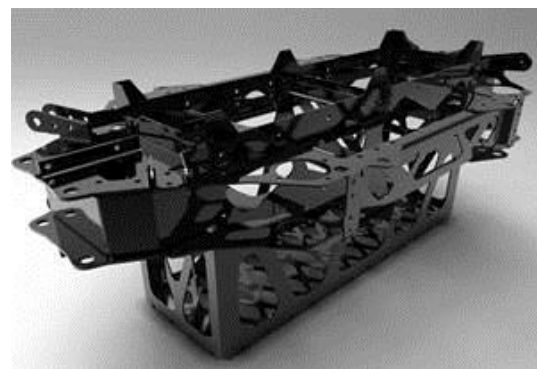


Fig. 4. A prototype of a mobile robot

The following construction assumptions were adopted in the calculations:

- the predicted mass of the platform mounted on the vehicle – $m_p = 50$ kg ($m_1 = 5$ kg vision system weight, $m_2 = 30$ kg lifting mechanism weight, $m_3 = 15$ kg- base and drives weight);
- vehicle weight $m = 60$ kg;
- vehicle's wheel diameter: $d = 0.362$ m
- maximum driving speed $V_{max} = 5 \div 10$ km/h (1.39 ÷ 2.78m/s)
- rolling resistance coefficient:
 $f_o = 0.02$ – a concrete,
 $f_o = 0.1$ – a sand;
- predicted angle of climbing hills $\alpha = 00 \div 100$

It was assumed that the vehicle's drive consists of four Maxon EC-ib2 + 6P52C engines driven by four batteries, each with a voltage of $U = 12$ V and a capacity of $Q = 18$ Ah.

Prepared calculations are aimed at determining the longitudinal and transverse stability of the designed mobile robot. In this section, in sequence the following calculations are presented:

- determining the traction properties of the "Trifid" system [3, 4];
- determining the centre of gravity of the mobile robot;
- determining the centre of gravity of the platform;
- determining the turning radius;
- determining the longitudinal stability conditions of the "Trifid" system [5];
- determining the transverse stability conditions of the "Trifid" system [5].

3.1. Determining the traction properties of the Trifid" system

Maxon EC-ib2 + 6P52C engine was selected for the vehicle, whose dynamic and kinematic parameters are respectively:

- $M_s = 14.55$ Nm- a nominal moment;
- $n_s = 93$ rpm- a nominal speed;
- $\eta_s = 0.75$ - a mechanical efficiency coefficient.

The value of mechanical and electrical power was calculated from dependence (1) and (2):

$$P_M = \frac{M_s n_s}{9550} 1000 = 141.7 [\text{W}] \quad (1)$$

$$P_E = \frac{P_M}{\eta_s} = 188.9 [\text{W}] \quad (2)$$

The maximum vehicle speed is determined from the following dependence:

$$V_p = \frac{\pi d n}{60} = 1.76 [\text{m/s}]. \quad (3)$$

The maximum driving force can be calculated based on the dependence (4):

$$F_{nmax} = \frac{2M_s i}{d} = \frac{P_M i}{V_p} = 321.55 [\text{N}] \quad (4)$$

where $i = 4$ (a number of engines).

In order to determine the power, torque, and acceleration, for various operational variants of the

vehicle, it was necessary to determine the resistance to motion. The minimum resistance force is calculated from the following formula:

$$F_o = F_t + F_w + F_b \quad (5)$$

where: F_t - rolling resistance, F_w - grade resistance, F_b - inertial force.

Calculating the F_o force, the air resistance was omitted (due to the lower vehicle speed).

The rolling resistance was calculated from the following relationship:

$$F_t = f_o (m + m_p) g \quad (6)$$

where: $g = 9.81$ m/s - acceleration of gravity.

The grade resistance is calculated from the following formula:

$$F_w = (m + m_p) g \sin[\alpha] \quad (7)$$

The inertia force is determined from the following formula:

$$F_b = (m + m_p) a_{max} \delta \quad (8)$$

where: $\delta = 1.8$ - a factor depending on the radius of the wheel.

Using the formulas from 4 to 8, it is possible to calculate the maximum acceleration (assuming that $F_n = F_{nmax} = F_o$):

$$a_{max} = \frac{F_n - g(m + m_p)(f_o + \sin[\alpha])}{(m + m_p)(1 + \delta)} \quad (9)$$

The required torque on a single wheel (11) and the power requirement (12) under specific driving conditions are determined for the instantaneous equilibrium $F_n = F_o$. At this state of force balance, according to the second principle of dynamics, the acceleration is equal to 0. Therefore, by transforming the dependence (9) one can determine the required driving force F_n (10):

$$F_n = g(m + m_p)(f_o + \sin[\alpha]) \quad (10)$$

Knowing the value of the required driving force, using formulas (11) and (12), the torque and power can be found:

$$M_w = \frac{F_n d}{2i} \quad (11)$$

$$P_w = \frac{F_n n_s}{2i 9550} 1000. \quad (12)$$

In table 1 the acceleration values, as well as the required torque and power for different operating conditions (a ground type, an angle of climbing hills), have been shown.

The calculations carried out show that for the assumed operating conditions, the vehicle engine was selected correctly. The engines will be powered by 4 batteries, each with a voltage of $U = 12$ V and a capacity of $Q = 18$ Ah.

$$t = \frac{nQU\eta_s}{iP_w} [\text{h}], \quad (13)$$

$$s = \frac{nQUV_p\eta_s}{iP_w} [\text{km}], \quad (14)$$

where: $n=4$ (a number of batteries), $i=4$ (number of engines), $V_p=6.34$ (maximum speed of the vehicle), w - power in selected driving conditions (Tab. 1).

Table 1. Calculated values of the required torque and power for different operating conditions

	$\alpha=0^\circ$	$\alpha=5^\circ$	$\alpha=10^\circ$
ground- a concrete, $f_o=0.02$			
$a_{max}[m/s^2]$	0.973	0.668	0.365
$M_w[N\ m]$	0.976	5.232	9.45
$P_w[W]$	9.51	50.95	92.08
ground - a sand, $f_o=0.1$			
$a_{max}[m/s^2]$	0.693	0.388	0.085
$M_w[N\ m]$	4.882	9.138	13.36
$P_w[W]$	47.551	88.99	130.1

Table 2. The values of the operating time and the range of the of the robot calculated for different operating conditions

	$\alpha=0^\circ$	$\alpha=5^\circ$	$\alpha=10^\circ$
Ground - a concrete, $f_o=0.02$			
t [h]	17.034	3.179	1.759
s [km]	108	20.158	11.154
ground- a concrete, $f_o=0.02$			
t [h]	3.406	1.820	1.245
s [km]	21.599	11.54	7.893

The predicted operating time and range of the vehicle are shown in Tab. 2.

3.2. Determining the center of gravity of the mobile robot

The main dimensions of the robot with a marked centre of gravity are shown in Fig. 5. Coordinates determining the location of the centre of gravity (in the Cartesian coordinate system, with the origin located at the point where the wheel comes into contact with the ground) were determined on the basis of the 3D model. They are respectively: $x_c=500$ mm, $y_c=368$ mm, $z_c=382$ mm

3.3. Determining the center of gravity of the platform

The centres of gravity of the robot and platform are located on the same line which is normal to the ground so the both coordinates of the centre of gravity of the platform - x_c and z_c - will be the same as the robot.

It is clear that y_{cp} coordinate is different (Fig.6) and can be calculated with the formula (15):

$$y_{cp} = \frac{m_1 H_{max/min} + m_2 (h + (H_{max/min} - h) / 2) + m_3 h}{m_p} \quad (15)$$

where: $h=654$ mm - the height of the robot.

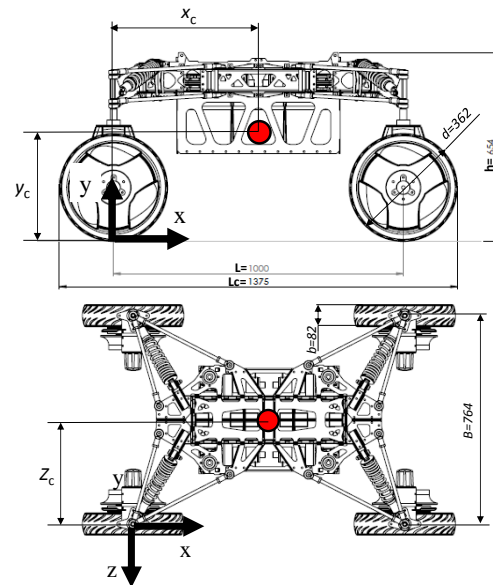


Fig. 5. The main dimensions of the robot with the marked centre of gravity, the front and top view

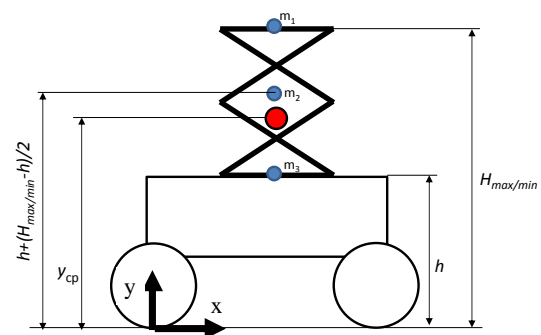


Fig. 6. The positions of the centre of gravity of platform

The positions of the centre of gravity determined for the expanded ($H_{max}=4954$ mm) and the folded platform ($H_{min}=1354$ mm) are equal:

$$y_{cp}(H_{max}) = 2374[\text{mm}], \quad y_{cp}(H_{min}) = 934[\text{mm}].$$

3.4. Determining the turning radius

By assumption, the robot can spin around in place (Fig. 7). Of course, it is possible to synchronize the drives for arc driving. It is necessary to specify the minimum radius at which transverse stability will be maintained. Therefore, the desired radius will be determined in the section on robot lateral stability.

The distribution of forces acting on the vehicle while driving uphill is shown in Fig. 8.

Based on the equation of moments' equilibrium in relation to the "O" point, a formula describing the normal reaction R_{py} (acting on the ground on the front axle) was obtained:

$$R_{py} = -\frac{\cos[\alpha](G+G_p)(e-x_c) + P_b y_c + P_{pb} y_{cp} + \sin[\alpha](G y_c + G_p y_{cp})}{L} \quad (16)$$

In the above formula, forces and geometric parameters are respectively:

$P_b = m a_{max}$ - an inertial force of the vehicle,
 $P_{pb} = m_p a_{max}$ - an inertial force of the platform,
 $G = mg$ - a gravity force of the vehicle, $G_p = m_p g$ - a gravity force of the platform, $e = f_o d / 2$ - shifting the reaction. In the calculations, it was assumed that a_{max} corresponds to the acceleration value of driving on a flat track (taking into account the type of the ground).

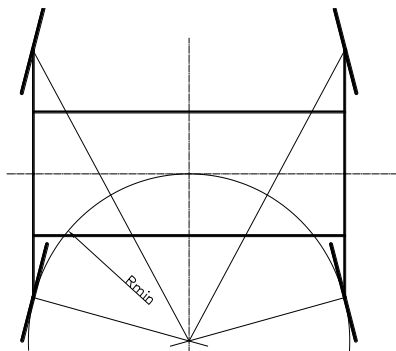


Fig. 7. The turning radius of the robot

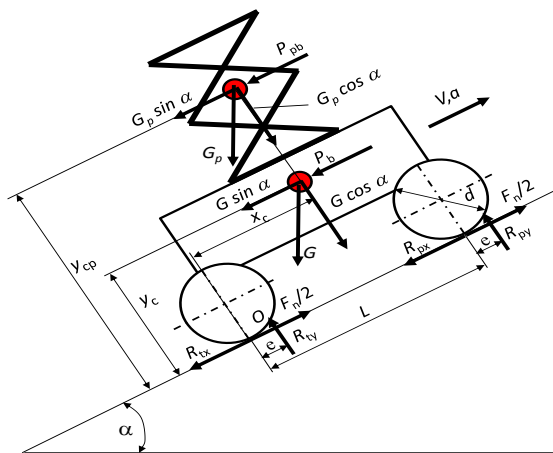


Fig. 8. The distribution of forces acting on the robot while driving uphill

The condition for maintaining the balance is that the reaction R_{py} should be greater than zero. In Fig. 9 ((a) driving on concrete and (b) driving on the sand, moving with an expanded platform) the value of the reaction to the ground depending on the inclination angle of the ground was graphically shown.

From the graph, it can be seen that for the movement with the expanded platform, the angle α cannot be greater than about 16° for driving on concrete and 16.85° when moving on sand. Similar calculations were made for a variant of moving with a folded platform. Permissible angles were: 33.5° for driving on concrete and 33.8° for moving on sand.

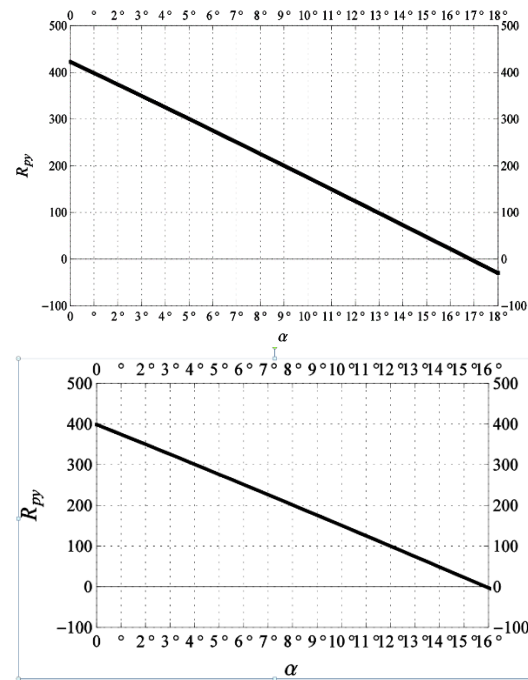


Fig. 9. The distribution of the normal front axle reaction to the ground depending on the angle of its, a) concrete ground, b) sand ground

3.6. Determining the transverse stability conditions of the Trifid's system

The distribution of forces acting on the vehicle while driving on an inclined surface is shown in Fig. 10. It was assumed that transverse stability must be maintained at the angle $\beta \leq 10^\circ$. The calculations consisted in determining the radius of the arc at which the robot can safely move.

$$R_{y2} = \frac{-2 \sin[\beta](G y_c + G_p y_{cp}) - 2(P_o y_c + P_{po} y_{cp}) + \cos[\beta](G + G_p)(b + 2z_c)}{b + 2B} \quad (17)$$

Similarly as in the problem of longitudinal stability, defining the equation of moments' equilibrium in relation to the "O" point, a formula (17) which describes the normal reaction acting on the ground was obtained. In the above formula, the forces and geometric parameters are respectively:
 $P_o = m V_{max}^2 / R$ - the centrifugal force of the vehicle,
 $P_{po} = m_p V_{max}^2 / R$ - the centrifugal force of the platform, R - the turning radius.

The necessary condition for maintaining the balance is that the reaction of R_{y2} must be greater than zero. Of course, transverse stability does not depend on the type of ground. In Fig. 11 the value of the reaction depending on the radius R was graphically presented.

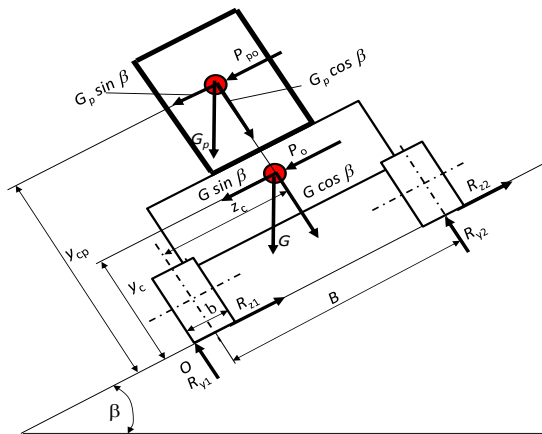


Fig. 10. Forces acting on a mobile robot in a transverse plane

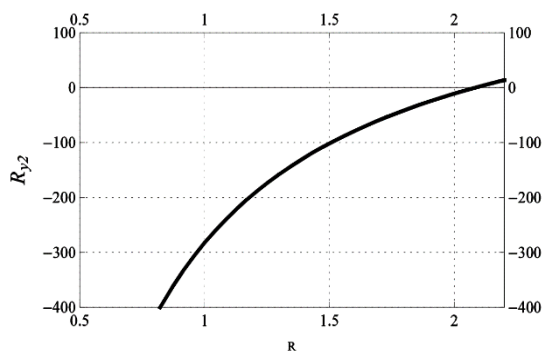
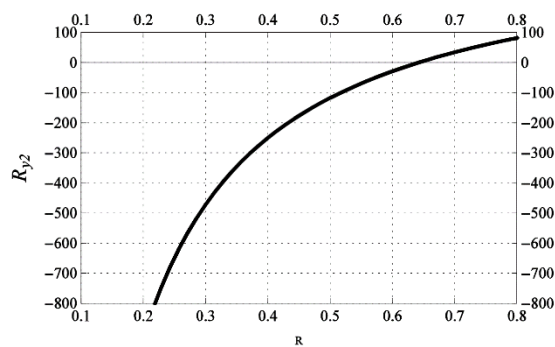


Fig. 11. Distribution of normal reaction on the ground (on one side of the robot) depending on the turning radius R a) platform expanded, b) platform folded

Based on the obtained results, it can be seen that the radius R cannot be less than about 2.08 m for the moving with an expanded platform and 0.63 m when the platform is folded.

A limiting angle β when the robot is spinning in place was also determined. It is obvious that with such robot's movement the centrifugal forces are equal to zero (the vehicle's speed of the centre point is zero). The limiting angles are equal respectively: $\beta = 18.2^\circ$, for movement with platform expanded, driving on concrete and sand; $\beta = 34.2^\circ$, for movement with platform folded, driving on concrete and sand.

4. Strength and durability analysis of the basic components of the "Trifid" system

As already mentioned, strength and durability calculations were carried out in two ways – analytically [6, 7] and numerically [8 - 10]. Their goal was to optimize the geometrical dimensions of individual components. For numerical calculations (finite element method), commercial software MSC.AFEA was used.

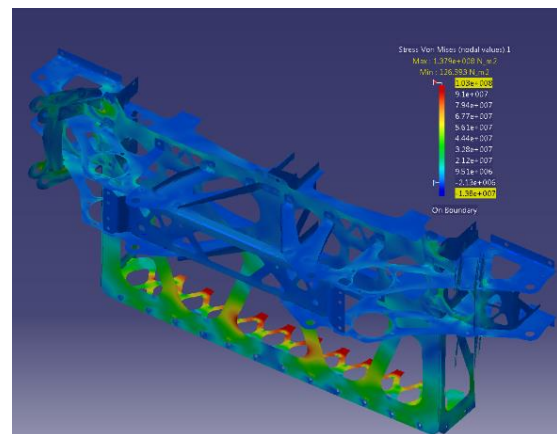
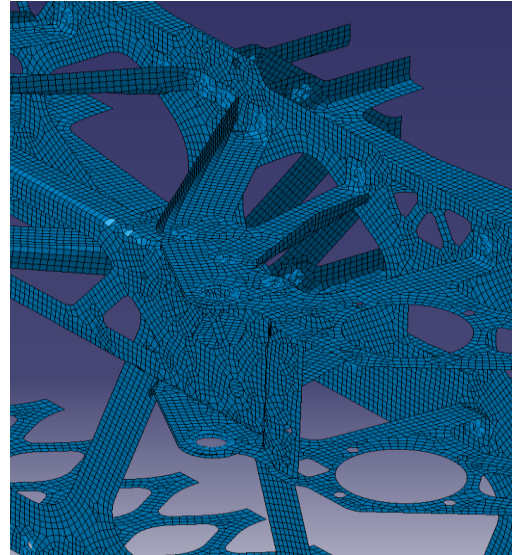


Fig. 12. Numerical modelling: a) a finite element mesh, b) a reduced stress

Based on the analyses carried out, it can be concluded that the structural elements meet load and rigidity conditions and safely transfer the assumed loads. In the calculations, exploitation accelerations (given in Tab. 1) were adopted, which reflected the normal operating conditions of the vehicle: starting and braking with the nominal engine power. Prepared calculations have not taken into account exceptional situations, such as hitting an obstacle or losing contact with the ground of one of the wheels. The mesh division and arbitrarily selected results of numerical calculations are presented in Fig. 12.

5. Lifting mechanism construction

The lifting mechanism (Fig.13) is mounted on the base of the platform (1). It consists of six segments- five moving (3) and one fixed (2). To obtain a vertical motion of the platform (lifting the platform) five pairs of belt transmissions are used. There is a friction between belts and segment guides (4) so the mutual displacement of segments is possible.

The pulleys are mounted on a fixed axis. The load on the transmission components results from the mass of the segment/segments which are lifted by it. The first transmission is the most loaded (looking at from the bottom of the platform), which has to lift 5 segments. The fifth (last) transmission is the least loaded because it moves only one segment. The masses of individual segments differs slightly, so in order to simplify the calculations, they are assumed to the same and are equal: $m_s = 3.2\text{kg}$. Due to the fact that identical elements were used in all transmissions calculations were made only for the first one (which is the most loaded).

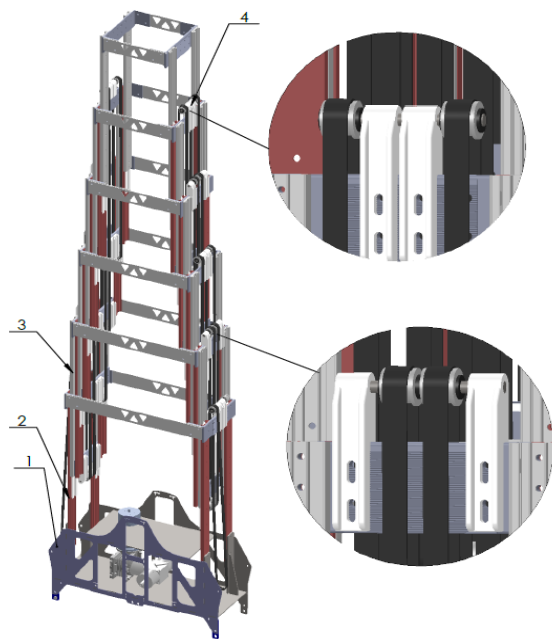


Fig. 13. The lifting mechanism in the extended position, 1. base with drives, 2. fixed segment, 3. moving segments, 4. segment guides.

The prepared calculations allow finding:

- the diameter of transmission's axis;
- the size and type of the transmission belt; (HDT 1420-5M-15 toothed belt) [11];
- the size and type of bearing; (self-lubricated slide bearing, made of iglidur [12]).

6. Summary

In this paper, the design procedures of the mechanical parts of the "Trifid" system were presented. The prepared analyses are related to:

- a review of existing solutions, which may constitute a source material that is an analysis of the state of the commercial solutions, especially in researching the patentability of mobile control systems,
- determining the traction properties of the device,
- determining the stability of the device for different driving conditions, including the maximum and minimum lifting of the platform;
- strength and durability analysis of the "Trifid" system's components.

References

- [1] Tetlow, K.: New Elevator Technology: The Machine Room-Less Elevator, (2007)
- [2] Advertising materials of the South Midlands Communication Ltd UKR.
- [3] Akopjan, P.A.: Construction of motor vehicles: construction and design of car suspension systems, Rzeszów University of Technology Publishing House, 1995 (in Polish).
- [4] Wong J. Y.: Theory of Ground Vehicles, Wiley, 2008
- [5] Arczyński S.: Mechanics of car movement. WNT, Warsaw, 1993 (in Polish).
- [6] Osiński Z.: Fundamentals of machine design. PWN, Warsaw, 2010 (in Polish).
- [7] Kaczyński R., Wilczewska I., Hościło B.: Construction analysis of mini-generator of electric energy using working medium flow as the working environment. Key Engineering Materials, Vol. 490, 2012, pp 45-53.
- [8] Zienkiewicz O. C., Taylor R. L., Zhu J. Z.: The Finite Element Method: Its Basis and Fundamentals, Butterworth-Heinemann, (2005).
- [9] Mieczkowski G.: Stress fields and fracture prediction for adhesively bonded bi-material structure with sharp notch located on the interface, Mechanics of Composite Materials, (2017),53,3, pp.305-320,
- [10] Mieczkowski G.: Optimization and Prediction of Durability and Utility Features of Three-Layer Piezoelectric Transducers, Mechanics, (2018),24,3,pp.335-342
- [11] PN-84/M-85212- Toothed belt transmissions - Calculations of transmission power and distance of wheel axles, Polish Standards,1984(in Polish)
- [12] <https://www.tme.eu/pl/katalog/?art=MFM-0408-08>